Enzyme and Microbial Technology 96 (2017) 163–169

Contents lists available at ScienceDirect

Enzyme and Microbial Technology

journal homepage: www.elsevier.com/locate/emt

Deciphering the factors defining the pH-dependence of a commercial glycoside hydrolase family 8 enzyme

Mário Barroca [a], Gustavo Santos [a], Björn Johansson [a], Florian Gillotin [b], Georges Feller [b], Tony Collins [a,*]

[a] Centre of Molecular and Environmental Biology (CBMA), Department of Biology, University of Minho, Campus de Gualtar, 4710-057 Braga, Portugal
[b] Laboratory of Biochemistry, Center for Protein Engineering, University of Liège, B-4000 Liège-Sart Tilman, Belgium

ARTICLE INFO

Article history:
Received 26 April 2016
Received in revised form 13 October 2016
Accepted 17 October 2016
Available online 17 October 2016

Keywords:
pH dependence
Activity
Stability
Solubility
Xylanase
Glycoside hydrolase family 8

ABSTRACT

A prerequisite to the use of any enzyme in any industrial process is an understanding of its activity and stability under process conditions. Glycoside hydrolase family 8 enzymes include many important biotechnological biocatalysts yet little is known of the performance of these with respect to pH. A better understanding of this parameter and its relationship to structure and function in these enzymes will allow for an improved use of these in industry as well as an enhanced ability in their engineering and optimisation for a particular application. An in-depth analysis of the pH induced changes in activity, irreversible inactivation, conformation, stability and solubility of a commercial glycoside hydrolase family 8 xylanase was carried out with the aim of identifying the factors determining the pH dependence of this enzyme. Our study showed that different phenomena play different roles at the various pHs examined. Both reversible and irreversible processes are involved at acidic pHs, with the irreversible processes dominating and being due to protein aggregation and precipitation. At basic pHs, loss of activity is principally due to reversible processes, possibly deprotonation of an essential catalytic residue, but at higher pHs, near the pI of the protein, precipitation again dominates while structure unfolding was discerned at the higher pHs investigated. Such insights demonstrate the complexity of factors involved in the pH dependence of proteins and advances our knowledge on design principles and concepts for engineering proteins. Our results highlight the major role of protein precipitation in activity and stability losses at both low and high pHs but it is proposed that different strategies be used in tailoring the enzyme to overcome this in each case. Indeed the detailed understanding obtained here will allow for a more focused, informed and hence successful tailoring of glycoside hydrolase family 8 proteins for a specific pH and process application.

1. Introduction

One of the principal challenges to the successful integration of an industrial biocatalyst into a commercial process is related to its fitness for the specific application. The enzyme needs to have the desired substrate specificity and selectivity and be highly active and stable under the process conditions. Frequently however, many naturally occurring enzymes do not fulfil all of these requirements, in particular as many industrial processes are carried out under harsh conditions such as extremes of temperature, pH, pressure, salinity and/or in the presence of organic solvents, detergents etc. [1,2]. Xylanases (*endo*-1,4-β-D-xylanase, E.C. 3.2.1.8) are important industrial biocatalysts regularly used in industrial processes in which extreme conditions prevail. They have found application in the technical, food and feed sectors of the enzymes market and are employed under such diverse extreme conditions as high temperatures (pulp and paper, bioconversion), low temperatures (food and beverages), acidic pHs (bioconversion, sulphite pulping, beverages, animal feed), alkaline pHs (bioconversion, kraft pulping, detergents) and/or even in the presence of detergents [3–9]. These enzymes randomly cleave the internal β-1,4-D-xylosidic linkages of the complex plant heteropolysaccharide xylan and are classified into glycoside hydrolase (GH) families 5, 7, 8, 10, 11 and 43 based on

Abbreviations: GH8, glycoside hydrolase family 8; pXyl, psychrophilic glycoside hydrolase family 8 xylanase (UniProtKB entry Q8RJN8); MOPS, 3-(*N*-morpholino)propanesulfonic acid; MES, 2-(*N*-morpholino)ethanesulfonic acid; TAPS, *N*-[Tris(hydroxymethyl)methyl]-3-aminopropanesulfonic acid; CHES, *N*-cyclohexyl-2-aminoethanesulfonic acid; CAPS, *N*-cyclohexyl-3-aminopropanesulfonic acid.

* Corresponding author.
E-mail address: tcollins@bio.uminho.pt (T. Collins).

http://dx.doi.org/10.1016/j.enzmictec.2016.10.011
0141-0229/

amino acid sequence similarity. Interestingly, while family 10 and 11 members have been extensively studied, much less is known about the other families' members [5,9,10].

We have previously isolated a glycoside hydrolase family 8 (GH8) xylanase, designated pXyl, from the Antarctic bacterium *Pseudoalteromonas haloplanktis* TAH3a [11] and extensively studied this at the physicochemical, functional and structural levels [12–15]. This was shown to be characterised by a specificity for xylan, being most active on long chain xylo-oligomers [11,16], and an insensitivity to xylanase inhibitors [17], as well as typical cold-adapted characteristics of a high activity at low to moderate temperatures and a reduced stability [13,18]. Importantly also, this enzyme has been successfully developed for use as a technological aid in baking where it allows for improved bread quality [19–21] and is currently being commercialised worldwide for use in this application. Indeed, the unique properties of this enzyme point to its suitability for exploitation in various other application areas, in particular in the beverages industry and in animal feeds but also, potentially, in biofuel production. In many of these applications extremes of pH are encountered yet, interestingly, while much is already known of this important industrial enzyme, little is known of its relationship to pH and of the pH dependence of its activity and stability. In fact, GH8 also contains many other industrially important enzymes such as cellulases, licheninases and chitosanases yet it appears that, in contrast to family 10 and 11 enzymes where a large number of studies have been carried out [5,9,10,22–26], pH adaptation in GH8 enzymes has not been studied. Furthermore, in contrast to adaptation of enzymes to temperature, and in particular high temperatures, much less is currently known of adaptation to pH, with variable and sometimes conflicting observations on adaptation strategies being reported [5,9,10,22–27].

Here we addressed these limitations by employing a variety of biochemical and biophysical techniques for an in-depth investigation of the pH dependence of the cold adapted GH8 xylanase pXyl. The detailed knowledge available for this enzyme; of its structure, function, activity and mechanism of action, as well as its commercial value, make it an attractive model for the study. The work described here enables a better understanding of adaptation to pH in this enzyme and in glycoside hydrolase family 8 enzymes in general, but also advances our knowledge on the factors defining the pH-dependent characteristics of enzymes, with important implications for protein science and protein engineering [28].

2. Material and methods

2.1. Xylanase production and purification

The pET22b(+)-*E. coli* BL21(DE3) expression system (Novagen) was used for overexpression of pXyl by batch production at 18 °C using previously described conditions [11] but with optimisation of the induction time and induction period. For optimisation, xylanase production levels following induction with 1 mM IPTG at various growth stages (mid-log, late-log and early-stationary phases) and various induction periods (0–24 h) were compared. Intracellular xylanase production levels were measured by activity measurements with a modified Bernfeld reducing sugar assay [29] with 3% soluble birchwood xylan and 0.1 M McIlvaine's buffer pH6.5, as described previously [11].

The xylanase was purified by a combination of anion exchange, cation exchange and gel filtration chromatographies (GE Healthcare Life Sciences) as previously described [11]. Purified enzyme was dialysed in storage buffer (pH 7.5, 20 mM MOPS + 100 mM NaCl) and stored at 4 °C until use. SDS-PAGE was employed for confirmation of protein purity.

2.2. Buffer mix

Throughout the study the following buffer mix covering the pH range from 3 to 12 was used: 100 mM Citrate (Merck), 20 mM MES (Sigma), 20 mM MOPS (Sigma), 20 mM TAPS (Sigma), 20 mM CHES (Sigma) and 20 mM CAPS (Sigma). The pH was adjusted with HCl or NaOH and the final pH of all solutions was measured after enzyme addition. Unless otherwise stated, all experiments were performed in triplicate.

2.3. pH dependence of activity

Activity of the purified protein as a function of pH was determined with the buffer mix described in 2.2 using a modified Bernfeld reducing sugar assay [29] with 3% soluble birchwood xylan as described previously [11] and assay times of 5, 30 and 60 min.

2.4. Irreversible inactivation

400 μg/mL purified xylanase was diluted 8-fold in the buffer mix at pHs from 3 to 12 and incubated at 25 °C. Samples were taken at 5 min and 24 h, diluted 8-fold in storage buffer (pH 7.5, 20 mM MOPS + 100 mM NaCl) and incubated for one hour at room temperature to allow for reversible refolding/reactivation. Residual activity was measured with a 5 min assay under optimal conditions (pH 6.5 in 0.1 M McIlvaine's buffer) with the Bernfeld reducing sugar assay as described in 2.3 [11,29].

2.5. Tertiary structure analysis: fluorescence spectroscopy

400 μg/mL purified xylanase was diluted 8-fold in the buffer mix at pHs from 3 to 12 and incubated at 25 °C. Samples were taken at 5 min and 24 h and fluorescence emission spectra recorded from 300–400 nm following excitation at 295 nm on a PerkinElmer LS50 fluorescence spectrometer with a scan rate of 100 nm/min and data interval of 0.5 nm. As controls, the fluorescence emission spectra of the xylanase following high temperature and guanidine hydrochloride treatment at pH 7.5 were also measured. The former was prepared by incubating the enzyme diluted in pH 7.5 buffer mix at 80 °C for 20 min before fluorescence spectroscopy analysis as described above. For the latter 6 M guanidine hydrochloride was included in the pH 7.5 buffer mix used for dilution.

2.6. Structural stability: thermal denaturation

400 μg/mL purified xylanase was diluted 8-fold in the buffer mix at pHs from 3 to 12 and incubated at 25 °C for 24 h. The fluorescence intensity at 343 nm with excitation at 280 nm was then measured during a temperature ramp from 25 °C to 70 °C at 1.5 °C/min. A PerkinElmer LS50 Fluorescence Spectrometer connected to a LKB BROMMA 2219 MultiTemp II thermostatic circulator was used. The temperature of the enzyme solution was measured throughout the fluorescence study and data were treated for determination of the denaturation temperature as described by Pace [30].

2.7. Protein solubility

200 μg/mL purified xylanase was incubated in the buffer mix at pHs from 3 to 12 for 24 h at 25 °C, centrifuged at 25000 × *g* for 30 min at 4 °C and supernatants analysed for soluble protein content by absorbance measurements at 280 nm on a UV–vis 1700 spectrophotometer (Shimadzu). To measure the effect of protein concentration on solubility, various concentrations of purified xylanase, from 0.07 to 3.6 mg/mL, in 20 mM MOPs buffer with 100 mM NaCl, pH 7.5 were prepared with an Amicon Ultra-15 Centrifugal Filter Unit, 10 KDa cut-off (Merck Millipore) and incubated

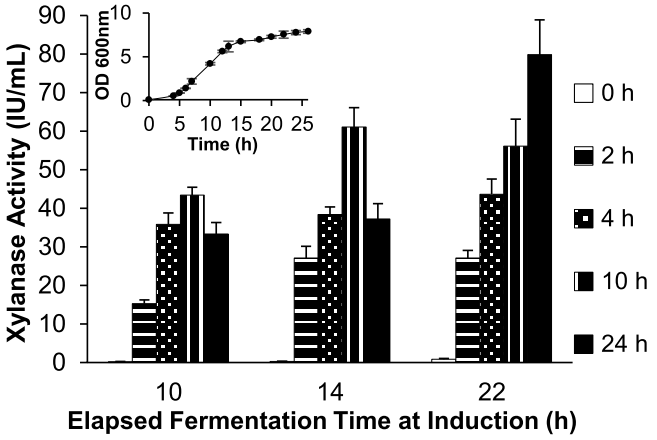

Fig. 1. Effect of elapsed fermentation time at induction and post-induction period on xylanase production. Comparison of xylanase production levels, expressed as international units (IU) of xylanase activity per mL of cell culture, as a function of the elapsed fermentation time at induction (10, 14 and 22 h incubation) and post-induction period (0–24 h). The inset graph shows the growth curve of uninduced *E.coli* BL21(DE3) for assessment of the elapsed fermentation time and stage of growth.

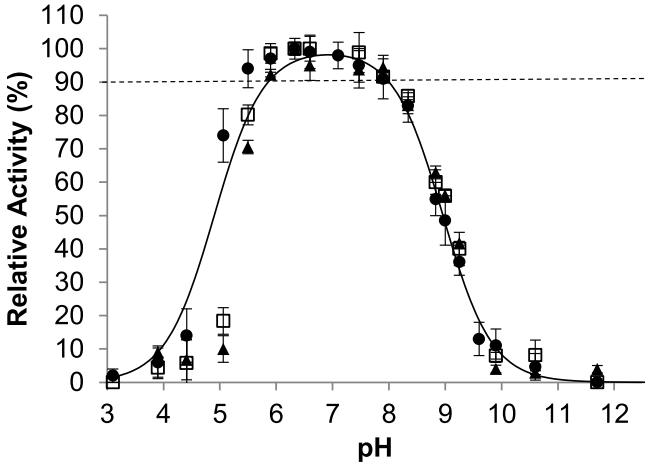

Fig. 2. pH activity profile for the glycoside hydrolase family 8 xylanase. Relative activities for 5 (filled circles), 30 (empty squares) and 60 (filled triangles) minute activity assays are shown. The dashed line indicates the 90% relative activity level. The solid line represents the fitting of the Henderson-Hasselbalch equation to the 5 min data.

at 25 °C. Samples were taken at 0 h and following 24, 72 and 168 h incubation and analysed for soluble protein content as described above.

3. Results and discussion

3.1. Xylanase production

The protein was produced and purified essentially as described previously [11] but with optimisation of the induction time and period. From Fig. 1 it can be seen that, under the conditions used, optimum pXyl production was obtained by induction with IPTG during the early stationary phase (following approximately 22 h incubation at 18 °C) for 24 h. This is in agreement with a recent comprehensive study of batch production approaches with the *E.coli*-pET expression system where it was shown that, in contrast to what is generally believed, optimal recombinant protein production is obtained by induction during the stationary phase [31]. Indeed, protein production is most commonly induced during the exponential growth phase when cells are most actively dividing [32] but our previous studies showed that induction during the stationary phase, where a higher cell density and possibly also a reduced stress on the cells is observed, enables for increased recombinant protein production [31,33]. In accordance with this, and further illustrating the advantages of the approach, in the present study we observed an almost doubling in xylanase production for induction during the stationary phase as compared to induction during the exponential phase. Finally, due to the cold-adapted characteristics and heat instability of the enzyme, an incubation temperature of 18 °C was used, with a resultant reduced growth rate for the *E. coli* host and hence, consequently, an extended induction period of approximately 24 h being required.

3.2. pH dependence of activity

The activity profile for the purified enzyme as a function of pH with 5, 30 and 60 min assays is shown in Fig. 2. Here, activity values greater than or equal to 90% are taken as reflecting a fully active state and it can be seen that under the conditions used optimum activity for pXyl is observed between pHs 5.5 and 8 for the 5 min assay and pHs 6 and 8.0 for the 60 min assay. Outside of this range a rapid loss of activity occurs.

GH8 enzymes catalyse hydrolysis with inversion of the anomeric configuration of the substrate with two catalytic residues, namely the proton donor and proton acceptor, playing essential roles. These two residues have been identified in pXyl as glutamic acid 78 (E78) and aspartic acid 281 (D281), respectively [12]. If one assumes that the pH-dependent activity of the enzyme is defined by the protonation/deprotonation of these two or indeed any two essential residues then the Henderson-Hasselbalch equation can be rearranged to describe this as follows:

$$\textit{Relative Activity}\,(\%) = \left(\frac{1}{1 + 10^{(pKa1 - pH)} + 10^{(pH - pKa2)}}\right) * 100 \qquad (1)$$

Fitting this equation to the 5 min data (filled circles) in Fig. 2 indicates good agreement of the bell shaped curve (black line) with the measured data at neutral and basic pHs while discrepancies are seen for the acidic limb. Such discrepancies indicate that the loss of activity observed at acidic pHs is due to something other than, or in addition to, protonation of an essential residue. Furthermore, it can be seen that use of longer assay periods (30–60 min) resulted in even steeper losses at acidic pHs, at pH 5.5 and below, while the relative activity for the basic limb was little changed. Indeed the pK_a of the residue involved in activity loss at basic pHs can be calculated from Eq. (1) but the poor agreement of data at the acidic pHs invalidates use of the acid pH data. A glutamic acid (E78), as the proton donor, is suggested as being the critical residue governing the basic pH limb in pXyl yet a pK_a of 9 was calculated from equation 1 even though the side chain carboxylic group of glutamic acid in solution has a reported pK_a of ~4.3. Nevertheless pK_a values can vary considerably depending on the environment [25] and in fact high pK_a values for acidic side chains are frequently reported, in particular for the catalytic residues of enzymes e.g. the acid/base residue in Xln A from *Streptomyces lividans* has a pK_a of 9.4 [34] while that of a glycoside hydrolase family 1 β-glucosidase has a pK_a of 8.1 [35]. Structural analysis of pXyl (pdb: 1H13, 1H14) indicates that E78 is located in the active site pocket near numerous hydrophobic (W82, Y380, Y381, W124, Y203) and acidic (D144, D281, D200) residues which could potentially stabilise the protonated form of the side chain and thereby increase the pK_a and allow for the high value observed. Thus taken together, these observations indicate that the loss of activity observed at high pHs may indeed be related to the reversible deprotonation of an essential residue, possibly the proton donor (E78). On the other hand, more complex and time

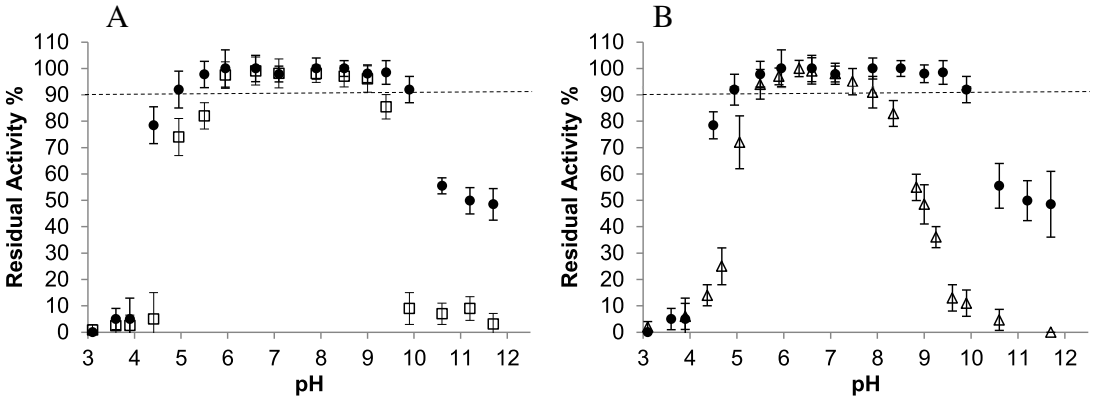

Fig. 3. Irreversible inactivation of the xylanase as a function of pH (A) and comparison of irreversible inactivation with activity (B). Residual activities following 5 min (filled circles) and 24 h (empty squares) incubation at various pHs are shown in (A). The five minute data for irreversible inactivation (filled circles) and activity (empty triangles) as a function of pH are compared in (B). The dashed line indicates the 90% level.

dependent factors, other than simply protonation of an essential residue, play a role in the loss of activity at acidic pHs.

3.3. Irreversible inactivation

Investigation of irreversible inactivation via measurement at optimum pH of the activity remaining after incubation at various pHs gives a measure of the stability of the activity of the enzyme. In this study two incubation periods were used; 5 min, for comparison with the 5 min activity assay, and 24 h, for determination of longer term effects on the enzyme. From Fig. 3A it can be seen that maximum (≥90 %) retention of activity occurs between pHs 5 and 10 following 5 min incubation and that this range is reduced to pHs 6–9 following 24 h. Thus at pHs below 6 and above 9 time dependent irreversible processes which negatively affect enzyme activity occur. Indeed these irreversible processes become dominant at the extremes of pH; at the low pH extremes complete irreversible inactivation already occurs after only 5 min incubation while at pH 10 and above irreversible inactivation dominates for the longer incubation period examined (24 h).

From Fig. 3B, where the results of the 5 min activity and inactivation studies are compared, it can be seen that the activity losses observed between pHs 5 and 10 are solely due to reversible processes as no significant irreversible inactivation was detected. Thus, as previously discussed, the activity loss observed for the basic pH limb, between pHs 8 and 10 with the 5 min assay, are solely due to reversible processes. On the other hand, above pH 10 and for the acidic pH limb at ~pH 4.5, it can be seen that the activity loss measured is greater than that due to irreversible inactivation alone and hence indicates that the observed loss of activity at these pHs is due to both reversible and irreversible processes.

As discussed earlier, the reversible processes at basic pHs likely involve deprotonation of the proton donor (E78) whereas those observed here at acidic pHs could involve protonation of the proton acceptor (D281) or, as previously described for a homologous family 8 chitosanase (ChoK), an irreversible repositioning of the proton donor at an inactive position at acidic pHs [36]. Interestingly, a similar position for the proton donor, near the nucleophilic water molecule, was reported for the wild-type pXyl crystal structure at pH 5 [15]. An induced fit mechanism wherein this proton donor is repositioned on substrate binding was suggested [14] but we propose that the E78 position observed was resultant of the low pH used and hence a crystal structure of wild type pXyl at neutral pHs (~pH 7) is called for. In contrast to the reversible processes, the factors involved in the irreversible processes are as yet unclear and hence, in an attempt to identify these, our studies were focused on characterising the effects of pH on the xylanase structure, stability and solubility.

3.4. Tertiary structure analysis: fluorescence spectroscopy

Fluorescence spectroscopy was used here to probe perturbations induced by pH in the folded state of the protein. The cold adapted xylanase contains 10 tryptophans, 30 tyrosines and 23

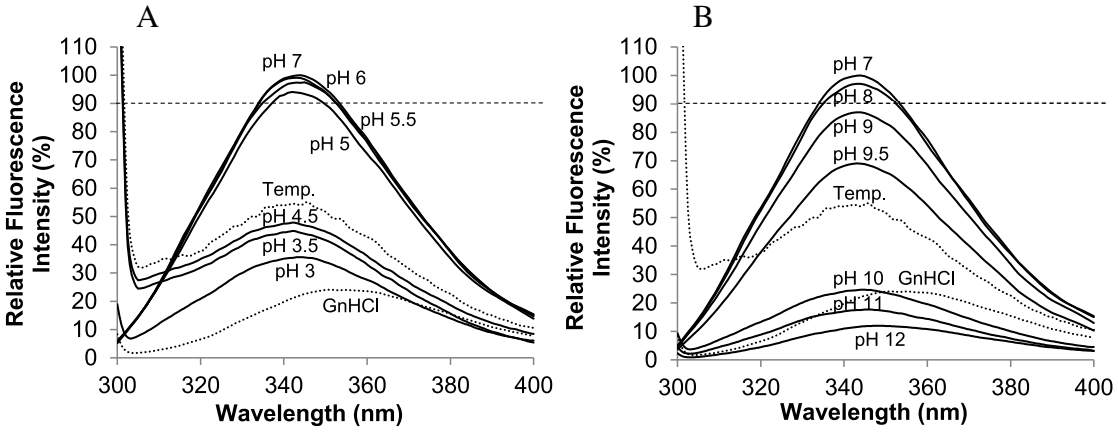

Fig. 4. Fluorescence emission spectra for the xylanase after 24 h incubation at various pHs. The results for incubation at low pHs (A) and high pHs (B) are shown (solid lines) as well as emission spectra for guanidine hydrochloride (GnHCl, dotted line) and temperature (Temp., dotted line) denatured protein. The horizontal dashed line indicates the 90% level.

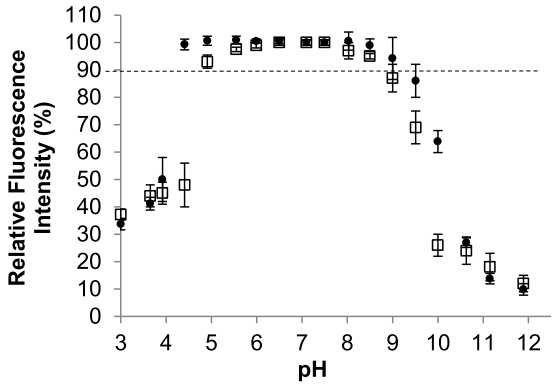

Fig. 5. Relative fluorescence intensity of the xylanase at 343 nm following 5 min (filled circle) and 24 h (empty square) incubation at various pHs. The horizontal dashed line indicates the 90% level.

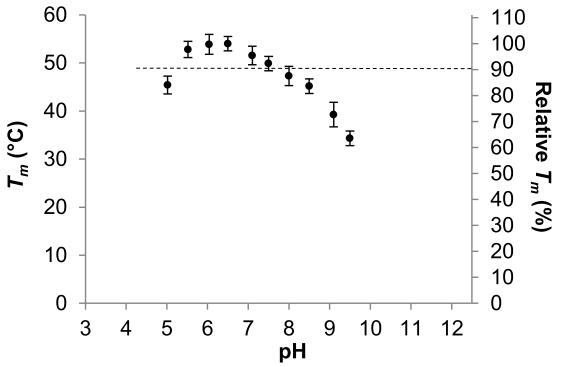

Fig. 6. Apparent denaturation temperature of the xylanase following 24 h incubation at various pHs. The measured apparent melting temperatures (T_m, left axis) and the values expressed as a percentage of the maximum at pH 6.5 (relative T_m, right axis) are shown. No transitions were observed following incubation at pHs ≤pH 4.5 or ≥pH 10. The horizontal dashed line indicates the 90% level.

phenylalanines but as tyrosine fluorescence can be affected by pH [37] and that of phenylalanine is relatively weak, focus was directed to the tryptophans via excitation at 295 nm. Structural analysis indicates that the 10 tryptophans of pXyl are distributed throughout the structure and analysis via the GETAREA server [38] indicates that 2 tryptophans (residues W124 and W249) are strongly exposed (>30% surface exposition), 5 are weakly exposed (5–30% exposition) and the remaining 3 are buried (<5% exposition).

From Figs. 4 and 5 it can be seen that no significant structural modifications were detected with this technique between pHs 4.5 and 9.5 after 5 min and pHs 5 and 9 after 24 h incubation. At pHs 4 (5 min incubation) and 4.5 (24 h incubation) an abrupt decrease in the fluorescence intensity to an acid denatured state with a residual relative fluorescence intensity of ∼50% occurs. In contrast, at the basic pH limb, a more gradual decrease in fluorescence intensity is initially observed at pHs 9 and 9.5 before a strong decrease at pH 10.5 (5 min incubation) or pH 10 (24 h incubation) and then again a more gradual reduction in fluorescence intensity to a denatured state at the higher pHs. The high pH (pH 11–12) denatured state is characterised by a drastically reduced fluorescence intensity and a slight shift in its emission maximum to higher wavelengths (348 nm, as compared to 344 nm at neutral pHs), somewhat similar to the guanidine hydrochloride unfolded protein and characteristic of a denatured state with little residual structure (Fig. 4). On the other hand, the high residual fluorescence for the acid denatured state at pHs 3.5–4.5 and minor shift to lower wavelengths is similar to the high temperature denatured sample (Fig. 4) and indicates an incompletely unfolded state in which the tryptophan residues are at least partially buried, suggestive of an aggregated or molten globule state.

3.5. Stability: thermal denaturation

The effect of pH on the stability of the protein was investigated by measuring the residual thermal stability following 24 h incubation at various pHs. Here thermal denaturation was found to be irreversible and led to protein precipitation. Hence the thermodynamic parameters of stability could not be calculated and only the apparent T_m, as a measure of the kinetics of the irreversible process under the conditions used, could be determined. From Fig. 6 it can be seen that, with an average apparent T_m of 53.9 °C, maximum stability was at pH 6 to 6.5 under the conditions used and that high relative protein stability (≥90% of maximum) was observed between pHs 5.5 and 7.5. Nevertheless, it is important to note that at this 90% level a more than 5 °C reduction in the apparent T_m is already observed, suggestive of a significantly increased rate for the irreversible process even at this level. Furthermore, reductions in the apparent T_m at acidic pHs down to pH 5 and more gradual reductions at the basic pH limb are followed by the absence of transitions for the samples at pH 4.5 and below and at pH 10 and above indicating that here the transition had already occurred during incubation at these pHs.

3.6. Protein solubility

The results of the protein solubility study are given in Fig. 7 where it can be seen that strong precipitation occurs at pHs ∼3.5–4.5 and ∼9.5–10.5. Such results show that the irreversible processes observed earlier at these pHs are dominated by protein precipitation but the increased solubility seen at more extreme pHs suggests that here protein unfolding becomes dominant. Thus the accentuated loss of activity, high irreversible inactivation, abrupt decrease in fluorescence intensity to a denatured state with a high residual relative fluorescence intensity as well as the lack of a thermal transition at acidic pHs (∼<pH 4.5) are all resultant of precipitation of the protein at these pHs. Furthermore, at the basic pHs, the irreversible inactivation observed above pH 9, the relatively high residual fluorescence intensity at ∼pH 10 and the absence of a thermal denaturation transition at this same pH are also due to protein precipitation. Interestingly ∼pH 10 is close to the isoelectric point of pXyl (pI = 9.5–10) where it possesses a net zero charge and where, as seen here, proteins in general tend to have a reduced solubility [39].

Precipitation has been previously observed for pXyl at high concentrations [40] and following heat denaturation [41] and here we investigated this further. Precipitation was found to be dependent

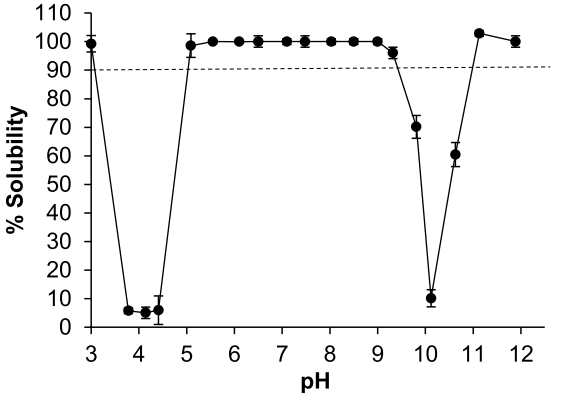

Fig. 7. Xylanase solubility as a function of pH. The concentration of protein remaining in solution was measured following 24 h incubation at various pHs. The horizontal dashed line indicates the 90% level.

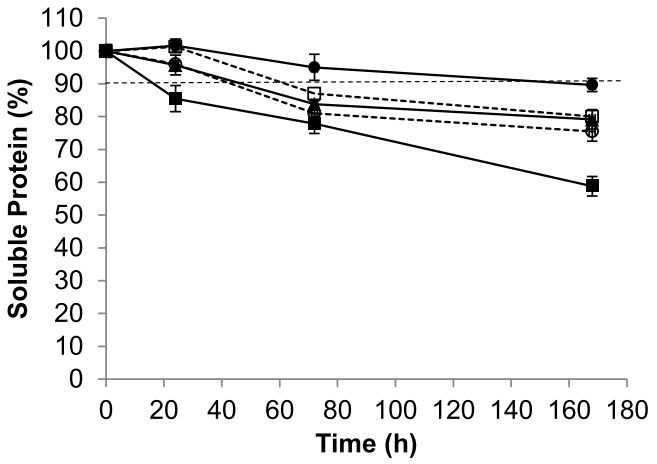

Fig. 8. Solubility of xylanase as a function of initial concentration and incubation time. Initial xylanase concentrations of 0.07 mg/mL (filled circles, solid line), 0.5 mg/mL (empty squares, dotted line), 1.4 mg/mL (filled triangles, solid line), 2 mg/mL (empty circles, dotted line) and 3.6 mg/mL (filled squares, solid line) were examined. The horizontal dashed line indicates the 90% level.

on the protein concentration (Fig. 8) and indeed turbid solutions were clearly visible at concentrations of 2 mg/mL and higher under the conditions used. Thus pXyl has a high propensity for precipitation with this being governed by both initial protein concentration and pH. Hydrophobic effects are believed to play a crucial role in promoting protein aggregation [42] and pXyl has already been reported as being characterised by a relatively high exposure of hydrophobic residues (16.7% of accessible surface area) [15]. This high surface hydrophobicity has been suggested as being related to its adaptation to low temperatures [15] but may also play a role in the high tendency of this enzyme to precipitate as seen here.

4. Conclusions

In this study we produced and purified a GH8 xylanase and carried out an in-depth analysis of the pH induced changes in activity, irreversible inactivation, conformation, stability and solubility so as to identify the factors determining the pH dependence of this industrial enzyme. Different optimal pH ranges were observed with each of the techniques used (see the recapitulative Fig. 9) which reflects both the diverse parameters measured and the distinct sensitivities of the techniques used and highlights the necessity of using a variety of different techniques when characterising proteins.

Highest activity and stability was seen at near neutral pHs and decreased with shifts towards both the acidic and basic pHs. At acidic pHs, the initial loss of activity is due to reversible processes, possibly a repositioning of the proton donor [36] or/and protonation of the proton acceptor, which have little effect on stability or are poorly detected by the techniques used. However, this is rapidly overcome by strong irreversible precipitation which develops over time, with a maximum at pH 4.5 leading to large alterations in all parameters measured. Analysis of the results for the basic pHs indicates that here a different phenomena occurs to that observed at acidic pHs. Initially, conformational alterations accompanied by a reversible loss of activity are observed and allows one to suggest that this may include a reversible deprotonation of the proton donor E78. Subsequently, at pH 10, close to the pI, protein precipitation leads to large modifications being detected in the structure and activity and is followed by protein unfolding at higher pHs leading to a denatured state with little residual structure.

The structure, function, solubility and stability of proteins at a given pH depend on their net charge and the charge state of the individual ionizable residues. Hence, most commonly, approaches for engineering proteins for increased activity and/or stability at acidic or basic pHs involve amino acid changes that alter the pK_a of specific residues, modify the surface charge and/or sometimes also introduce stabilising interactions. From this study it can be appreciated that such approaches would probably have little effect with this GH8 enzyme. At acidic pHs protein precipitation dominates and would mask any positive effects resultant of an engineering strategy focused on activity or stability. Here focus should be placed on reducing precipitation, namely by reducing the surface hydrophobicity via mutation of surface hydrophobic residues to polar residues [43]. At basic pHs, mutations aiming at altering the environment of the proton donor E78 to increase its p*Ka* would probably be effective but at pHs close to 10 precipitation again becomes dominant. This is probably resultant of the net zero charge on the protein near its pI and hence approaches for alleviating precipitation here should be focused on increasing the net charge on the protein at this pH [39]. Finally, at even higher pHs, protein unfolding dominates and hence introduction of stabilising interactions may be relevant.

The insights obtained in this study have implications in protein science and protein engineering and demonstrate the complexity and various factors associated with the pH dependence of proteins and the engineering of these. The identification and detailed description of the various factors determining the pH dependence of pXyl allows for a better understanding of this enzyme and of GH8 enzymes in general and will enable for a more successful tailoring and optimisation of these to a specific process condition.

Conflict of interest

The authors declare that they have no conflict of interest.

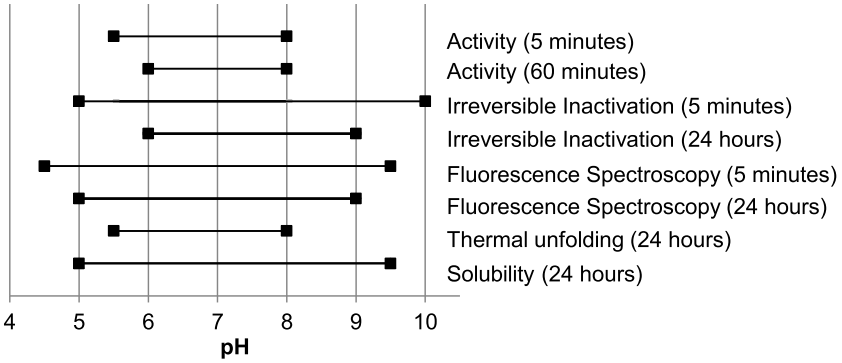

Fig. 9. Summary of the results obtained for pXyl. The optimum pH range (≥90% of the maximum) determined for the activity, irreversible inactivation, stability (fluorescence spectroscopy, thermal unfolding) and solubility are shown.

Author contributions

MB and TC conceived and designed the study and participated in its implementation. MB, GS, BJ, FG, GF and TC carried out the experimental studies. All authors have seen the manuscript and approved its submission.

Acknowledgements

This work was financed by FEDER through POFC-COMPETE and by the Fundação para a Ciência e Tecnologia (FCT) through project EngXyl (EXPL/BBB-BIO/1772/2013 – FCOMP-01-0124-FEDER-041595) as well as through strategic funding via UID/BIA/04050/2013 (POCI-01-0145-FEDER-007569) and by the ERDF through Compete 2020 – POCI. G.F. is supported by the Belgian program of Interuniversity Attraction Poles (iPros P7/44). M.B. acknowledges the FCT for grant PD/BD/113810/2015 within the Doctoral Program in Applied and Environmental Microbiology. T.C. is supported by the FCT, the European Social Fund, the Programa Operacional Potencial Humano and the Investigador FCT Programme (IF/01635/2014).

References

[1] A.S. Bommarius, M.F. Paye, Stabilizing biocatalysts, Chem. Soc. Rev. 42 (2013) 6534–6565.
[2] M.J. Liszka, M.E. Clark, E. Schneider, D.S. Clark, Nature versus nurture: developing enzymes that function under extreme conditions, Annu. Rev. Chem. Biomol. Eng. 3 (2012) 77–102.
[3] O. Akpinar, K. Erdogan, S. Bostanci, Enzymatic production of xylooligosaccharide from selected agricultural wastes, Food Bioprod. Process 87 (2009) 145–151.
[4] F. Beltramino, C. Valls, T. Vidal, M.B. Roncero, Exploring the effects of treatments with carbohydrases to obtain a high-cellulose content pulp from a non-wood alkaline pulp, Carbohydr. Polym. 133 (2015) 302–312.
[5] V. Juturu, J.C. Wu, Microbial xylanases: engineering, production and industrial applications, Biotechnol. Adv. 30 (2012) 1219–1227.
[6] V. Kumar, J. Marín-Navarro, P. Shukla, Thermostable microbial xylanases for pulp and paper industries: trends, applications and further perspectives, World J. Microbiol. Biotechnol. 32 (2016) 1–10.
[7] H. Li, X. Gao, J.D. Demartini, R. Kumar, C.E. Wyman, Application of high throughput pretreatment and co-hydrolysis system to thermochemical pretreatment. Part 2: dilute alkali, Biotechnol. Bioeng. 110 (2013) 2894–2901.
[8] K.K. Wong, L.A. Martin, F.M. Gama, J.N. Saddler, E. de Jong, Bleach boosting and direct brightening by multiple xylanase treatments during peroxide bleaching of kraft pulps, Biotechnol. Bioeng. 54 (1997) 312–318.
[9] T. Collins, C. Gerday, G. Feller, Xylanases, xylanase families and extremophilic xylanases, FEMS Microbiol. Rev. 29 (2005) 3–23.
[10] W. Bai, C. Zhou, Y. Zhao, Q. Wang, Y. Ma, Structural insight into and mutational analysis of family 11 xylanases: implications for mechanisms of higher pH catalytic adaptation, PLoS One 10 (2015) e0132834.
[11] T. Collins, M.A. Meuwis, I. Stals, M. Claeyssens, G. Feller, C. Gerday, A novel family 8 xylanase, functional and physicochemical characterization, J. Biol. Chem. 277 (2002) 35133–35139.
[12] T. Collins, D. De Vos, A. Hoyoux, S.N. Savvides, C. Gerday, J. Van Beeumen, G. Feller, Study of the active site residues of a glycoside hydrolase family 8 xylanase, J. Mol. Biol. 354 (2005) 425–435.
[13] T. Collins, M.A. Meuwis, C. Gerday, G. Feller, Activity, stability and flexibility in glycosidases adapted to extreme thermal environments, J. Mol. Biol. 328 (2003) 419–428.
[14] D. De Vos, T. Collins, W. Nerinckx, S.N. Savvides, M. Claeyssens, C. Gerday, G. Feller, J. Van Beeumen, Oligosaccharide binding in family 8 glycosidases: crystal structures of active-site mutants of the beta-1,4-xylanase pXyl from *Pseudoaltermonas haloplanktis* TAH3a in complex with substrate and product, Biochemistry 45 (2006) 4797–4807.
[15] F. Van Petegem, T. Collins, M.A. Meuwis, C. Gerday, G. Feller, J. Van Beeumen, The structure of a cold-adapted family 8 xylanase at 1.3 A resolution. Structural adaptations to cold and investgation of the active site, J. Biol. Chem. 278 (2003) 7531–7539.
[16] A. Pollet, J. Schoepe, E. Dornez, S.V. Strelkov, J.A. Delcour, C.M. Courtin, Functional analysis of glycoside hydrolase family 8 xylanases shows narrow but distinct substrate specificities and biotechnological potential, Appl. Microbiol. Biotechnol. 87 (2010) 2125–2135.
[17] E. Dornez, P. Verjans, F. Arnaut, J.A. Delcour, C.M. Courtin, Use of psychrophilic xylanases provides insight into the xylanase functionality in bread making, J. Agric. Food Chem. 59 (2011) 9553–9562.
[18] T. Collins, S. D'Amico, J. Marx, G. Feller, C. Gerday, Cold-adapted enzymes, in: C. Gerday, N. Glansdorff (Eds.), Physiology and Biochemistry of Extremophiles, ASM Press, Washington, D.C, 2007, pp. 165–179.
[19] T. Collins, G. Feller, C. Gerday, M.A. Meuwis, Family 8 enzymes with xylanolytic activity, in USPTO Patent (Granted): US8309336 B2 (2012).
[20] T. Collins, A. Hoyoux, A. Dutron, J. Georis, B. Genot, T. Dauvrin, F. Arnaut, C. Gerday, G. Feller, Use of glycoside hydrolase family 8 xylanases in baking, JCS 43 (2006) 79–84.
[21] A. Dutron, J. Georis, B. Genot, T. Dauvrin, T. Collins, A. Hoyoux, G. Feller, Use of family 8 enzymes with xylanolytic activity in baking, in Patents (Granted): US8192772 (2012), EP1549147B1 (2011), CN1681392B (2010), DE60336153 D1 (2011).
[22] B. Al Balaa, K. Brijs, K. Gebruers, J. Vandenhaute, J. Wouters, I. Housen, Xylanase XYL1p from *Scytalidium acidophilum*: site-directed mutagenesis and acidophilic adaptation, Bioresour. Technol. 100 (2009) 6465–6471.
[23] Y.C. Chen, Y.C. Chiang, F.Y. Hsu, L.C. Tsai, H.L. Cheng, Structural modeling and further improvement in pH stability and activity of a highly-active xylanase from an uncultured rumen fungus, Bioresour. Technol. 123 (2012) 125–134.
[24] S. Pokhrel, J.C. Joo, Y.H. Kim, Y.J. Yoo, Rational design of a *Bacillus circulans* xylanase by introducing charged residue to shift the pH optimum, Process Biochem. 47 (2012) 2487–2493.
[25] M.D. Joshi, G. Sidhu, J.E. Nielsen, G.D. Brayer, S.G. Withers, L.P. McIntosh, Dissecting the electrostatic interactions and pH-dependent activity of a family 11 glycosidase, Biochemistry 40 (2001) 10115–10139.
[26] G. Mamo, M. Thunnissen, R. Hatti-Kaul, B. Mattiasson, An alkaline active xylanase: insights into mechanisms of high pH catalytic adaptation, Biochimie 91 (2009) 1187–1196.
[27] T. Beliën, I.J. Joye, J.A. Delcour, C.M. Courtin, Computational design-based molecular engineering of the glycosyl hydrolase family 11 B. subtilis XynA endoxylanase improves its acid stability, Protein Eng. Des. Sel. 22 (2009) 587–596.
[28] Y. Li, P.C. Cirino, Recent advances in engineering proteins for biocatalysis, Biotechnol. Bioeng. 111 (2014) 1273–1287.
[29] P. Bernfeld, Amylases, α and β, Methods Enzymol. 1 (17) (1955) 149–158.
[30] C.N. Pace, Measuring and increasing protein stability, Trends Biotechnol. 8 (1990) 93–98.
[31] T. Collins, J. Azevedo-Silva, A. da Costa, F. Branca, R. Machado, M. Casal, Batch production of a silk-elastin-like protein in *E. coli* BL21(DE3): key parameters for optimisation, Microb. Cell Fact. 12 (2013) 21.
[32] J. Sambrook, D.W. Russell, Molecular Cloning A Laboratory Manual, 3rd ed., Cold Spring Harbor Laboratory Press, New York, 2001.
[33] T. Collins, M. Barroca, F. Branca, J. Padrao, R. Machado, M. Casal, High level biosynthesis of a silk-elastin-like protein in *E. coli*, Biomacromolecules 15 (2014) 2701–2708.
[34] F. De Lemos Esteves, T. Gouders, J. Lamotte-Brasseur, S. Rigali, J.M. Frere, Improving the alkalophilic performances of the Xyl1 xylanase from *Streptomyces* sp. S38: structural comparison and mutational analysis, Protein Sci. 14 (2005) 292–302.
[35] J.E. Nielsen, T.V. Borchert, G. Vriend, The determinants of alpha-amylase pH-activity profiles, Protein Eng. 14 (2001) 505–512.
[36] W. Adachi, Y. Sakihama, S. Shimizu, T. Sunami, T. Fukazawa, M. Suzuki, R. Yatsunami, S. Nakamura, A. Takenaka, Crystal structure of family GH-8 chitosanase with subclass II specificity from *Bacillus* sp. K17, J. Mol. Biol. 343 (2004) 785–795.
[37] J.R. Lakowicz, Protein fluorescence, in: J.R. Lakowicz (Ed.), Principles of Fluorescence Spectroscopy, Springer, Boston, MA, US, 2006, pp. 529–575.
[38] R. Fraczkiewicz, W. Braun, Exact and efficient analytical calculation of the accessible surface areas and their gradients for macromolecules, J. Comput. Chem. 19 (1998) 319–333.
[39] K.L. Shaw, G.R. Grimsley, G.I. Yakovlev, A.A. Makarov, C.N. Pace, The effect of net charge on the solubility, activity, and stability of ribonuclease Sa, Protein Sci. 10 (2001) 1206–1215.
[40] F. Van Petegem, T. Collins, M.A. Meuwis, C. Gerday, G. Feller, J. Van Beeumen, Crystallization and preliminary X-ray analysis of a xylanase from the psychrophile *Pseudoalteromonas haloplanktis*, Acta Crystallogr. D: Biol. Crystallogr. 58 (2002) 1494–1496.
[41] T. Collins, S. D'Amico, D. Georlette, J.C. Marx, A.L. Huston, G. Feller, A nondetergent sulfobetaine prevents protein aggregation in microcalorimetric studies, Anal. Biochem. 352 (2006) 299–301.
[42] J. Gsponer, M. Vendruscolo, Theoretical approaches to protein aggregation, Protein Pept. Lett. 13 (2006) 287–293.
[43] S.R. Trevino, J.M. Scholtz, C.N. Pace, Amino acid contribution to protein solubility: Asp, Glu, and Ser contribute more favorably than the other hydrophilic amino acids in RNase Sa, J. Mol. Biol. 366 (2007) 449–460.